# Molecular Docking, Synthesis and *In Vitro* Antiplasmodium Assay of Monoketone Curcumin Analogous from 2-Chlorobenzaldehyde

**Chessy Rima Mustika, Endang Astuti*, and Muhammad Idham Darussalam Mardjan**

*Department of Chemistry, Faculty of Mathematics and Natural Sciences, Universitas Gadjah Mada, Sekip Utara, Yogyakarta 55281, Indonesia*

* ***Corresponding author:***

*email: endangastuti@ugm.ac.id*

*Received: January 9, 2023*
*Accepted: May 22, 2023*

**DOI:** 10.22146/ijc.81122

***Abstract:*** *This research aimed to develop new curcumin analogous as antiplasmodium candidates. Six curcumin analogous (**1**-**6**) were proposed and docked against three* Plasmodium falciparum *receptors, namely PfENR, PfLDH, and PfATP6. The docking studies were carried out to predict the interaction among the compounds and receptors as well as their binding affinity. Three curcumin analogous (**3**, **4**, and **6**), which displayed specific interactions with the target receptors and possessed the lowest binding affinity were further proceeded to synthesis and* in vitro *antiplasmodium assay. Synthesis of the analogous **3**, **4**, and **6** was carried out from 2-chlorobenzadehyde* via *aldol condensation reaction and the products were obtained in good yields. Their* in vitro *antiplasmodium activities were then evaluated against* P. falciparum *FCR3 and 3D7 strains. The results showed that analogous **3**, **4**, and **6** were active against both strains with low levels of resistance. The* in silico *evaluation of the physicochemical and pharmacokinetic parameters showed that curcumin analogous displayed a better ADMET profile than curcumin, demonstrating the great potential of the developed curcumin analogous as antiplasmodium candidates.*

***Keywords:*** *aldol condensation; antiplasmodium; curcumin analogous; molecular docking; 2-chlorobenzaldehyde*

## ■ INTRODUCTION

Malaria is a serious parasitic disease and endemic in 85 countries. In 2020, the World Health Organization (WHO) reported that the number of malaria cases and mortality reached 241 million and 627 thousand, respectively. Malaria is caused by *Plasmodium* parasites. *Plasmodium falciparum* was reported as the deadliest species to humans and led to more than 90% of malaria cases in the world [1]. Several drugs have been developed to treat malaria, such as chloroquine, pyrimethamine, sulfadoxine, mefloquine and artemisinin. However, the resistance of the drugs against the *Plasmodium* parasite has been reported [2]. Hence, the development of new antiplasmodium agents is urgently required.

Curcumin is one of the natural compounds that has been reported to have many bioactivities such as anticancer, antidiabetic, anti-inflammatory, antiviral, antimicrobial, antioxidant, and antiplasmodium [3]. A previous study showed that curcumin extract has good *in vitro* antiplasmodium activity with an $IC_{50}$ value of 3.5 μg/mL [4]. Apart from the interesting biological activities, the applications of curcumin as a drug were limited due to its low bioavailability. The presence of unstable methylene and β-diketone groups in the structure of curcumin led to poor absorption, a high rate of metabolism, inactivity of metabolic products and rapid elimination from the body [3,5]. One of the strategies to improve curcumin bioavailability was by modifying the β-diketone group of curcumin into the monoketone group [6].

A number of strategies have been developed to synthesize monoketone curcumin analogous, such as through the aldol condensation reaction from aryl aldehydes and ketones in the presence of acid or base catalysts [7]. Aher and co-worker [8] reported that the synthesis of curcumin is analogous to acetone. They also

demonstrated that introducing a chloro substituent at the *ortho* position could improve the antimalarial activity against chloroquine-sensitive (3D7) and chloroquine-resistant (RKL9) strains of *P. falciparum* and could give a low resistance index. Previous studies also reported that coupling 2-chlorobenzaldehyde with various ketones such as *N*-methyl-4-piperidone, 4-piperidone, and cyclohexanone could generate bioactive curcumin analogous with anticancer, antibacterial and antiparasitic activities, respectively [9-11].

Several metabolic and biochemical pathways of the parasite should be considered during the design of new curcumin analogous to antiplasmodium agents. In this context, the protein targets involved in the pathways include enoyl-acyl carrier protein reductase (P*f*ENR), lactate dehydrogenase (P*f*LDH), and calcium ATPase (P*f*ATP6) [12]. Therefore, we initially introduced six curcumin analogous to molecular docking against key proteins of P*f*ENR, P*f*LDH, and P*f*ATP6. Three curcumin analogous possessing the lowest binding affinity and specific interaction with the three target receptors were then synthesized through the aldol condensation reaction. All the synthesized compounds were evaluated for their antiplasmodium activities against chloroquine-sensitive (3D7) and chloroquine-resistant (FCR3) *P. falciparum*. The *in silico* evaluation of physicochemical and pharmacokinetic properties, such as absorption, distribution, metabolism, elimination, and toxicity (ADMET) was also carried out.

## ■ EXPERIMENTAL SECTION

### Materials

The curcumin analogous used for the molecular docking study were (1*E*,4*E*)-1,5-bis(2-chlorophenyl)penta-1,4-dien-3-one (**1**), 2,5-bis((*E*)-2-chlorobenzylidene)cyclopentan-1-one (**2**), 2,6-bis((*E*)-2-chlorobenzylidene)cyclohexan-1-one (**3**), 3,5-bis((*E*)-2-chlorobenzylidene)piperidin-4-one (**4**), 3,5-bis((*E*)-2-chlorobenzylidene)-1-methylpiperidin-4-one (**5**), and 1-benzyl-3,5-bis((*E*)-2-chlorobenzylidene)piperidin-4-one (**6**) (Fig. 1).

The reagents and solvents used for the synthesis of curcumin analogous were 2-chlorobenzaldehyde, *N*-benzyl-4-piperidone, and 4-piperidone monohydrate hydrochloride from Macklin. Cyclohexanone, hydrochloric acid, glacial acetic acid, sodium hydroxide, ethanol and methanol were purchased from Merck. All reagents and solvents were analytical grades and used without further purification. Materials for *in vitro* antiplasmodium assay were microwell plate 96, RPMI-1640, red blood cell (RBC), serum-blood, dimethyl sulfoxide (DMSO), and curcumin.

### Instrumentation

The structure elucidation of curcumin analogous was performed using thin layer chromatography scanner (CAMAG TLC Scanner), Fourier transform infra-red spectrophotometer (FTIR, Shimadzu Prestige-21), high-resolution mass spectrometer (HRMS/MS, Waters Xevo

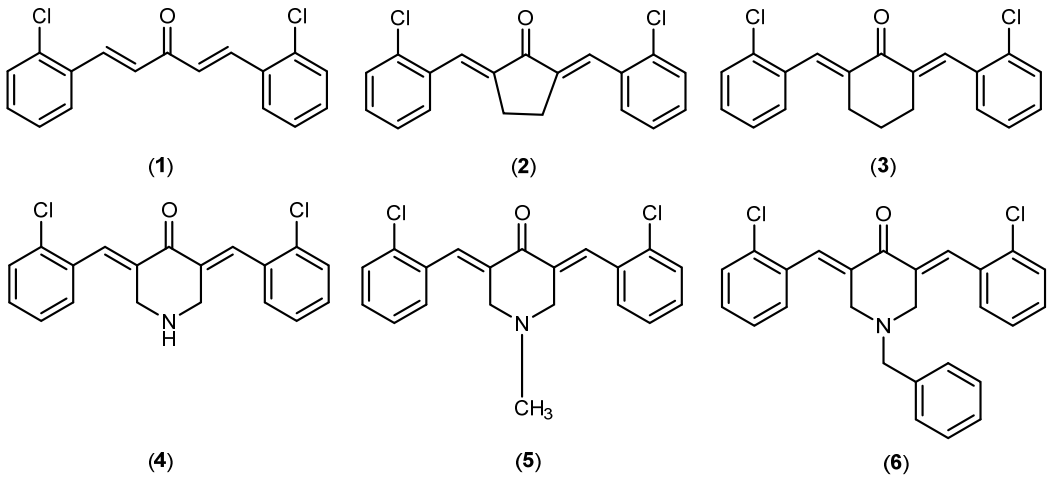


**Fig 1.** Chemical structure of curcumin analogous **1**-**6**

QtoF MS), and nuclear magnetic resonance spectrometer ($^1$H-NMR 500 MHz and $^{13}$C-NMR 125 MHz, JEOL JNMECA, with an internal standard of TMS). Moreover, the melting point was determined using the electrothermal 9100 melting-point apparatus.

## Procedure

### *Molecular docking of curcumin analogous*

The 3D structure of curcumin analogous **1**-**6** and curcumin was modelled using GaussView 5.0 and optimized with the semiempirical method of PM6 using Gaussian 09W. The crystal structures of the P*f*ENR (PDB ID: 1NHG), P*f*LDH (PDB ID: 1CET), and P*f*ATP6 (PDB ID: 1U5N) receptors were downloaded from Protein Data Bank. Each receptor was prepared using Chimera 1.15. The docking analysis was conducted with AutoDock 4.2.6. [13] using a Lamarckian Genetic Algorithm (LGA) followed by 50 times running. The grid box of P*f*ENR was 60 × 60 × 60 Å with 0.375 spacing. The most suitable conformation was selected from the lowest binding affinity. The visualization of the docking result was done using Discovery Studio Visualizer (DSV) 2021. The same procedure was used for P*f*LDH with the grid box of 45 × 45 × 45 Å, whereas the grid box size of P*f*ATP6 refers to research conducted by Dohutia et al. [14].

### *Synthesis of curcumin analogous*

**Synthesis of 2,6-bis((*E*)-2-chlorobenzylidene)cyclohexan-1-one (3).** Compound **3** was prepared using the procedure as in the previous report [11] with slight modifications. The 2-chlorobenzaldehyde (0.45 mL, 4 mmol) and cyclohexanone (0.21 mL, 2 mmol) were dissolved in ethanol (10 mL). The solution was stirred at room temperature for 15 min. Next, the aqueous solution of sodium hydroxide (40%, 3 mL) was added, and the reaction mixture was stirred at room temperature for 3 h. The reaction was quenched by adding the diluted hydrochloric acid solution. The yellow solid obtained was then filtered and washed with distilled water. Finally, the crude product was recrystallized from hot ethanol. Yellow solid; yield: 76%; purity: 100%; m.p.: 111–112 °C; FTIR (cm$^{-1}$): 2905 ($C_{sp^3}$–H), 1661 (C=O), 1433 (Ar C=C), 732 (C–Cl); $^1$H-NMR ($CDCl_3$, 500 MHz) δ (ppm): 1.75 (*m*, 2H, $CH_2$), 2.76 (*t*, *J* = 4 Hz, 4H, $CH_2$), 7.29 (*m*, 4H, $H_{Ar}$), 7.32 (*m*, 2H, $H_{Ar}$), 7.43 (*m*, 2H, $H_{Ar}$), 7.90 (*s*, 2H, CH=C); $^{13}$C-NMR ($CDCl_3$, 125 MHz); δ (ppm): 23.2 ($CH_2$), 28.5 ($CH_2$), 126.3 ($C_{Ar}$), 129.6 ($C_{Ar}$), 129.9 ($C_{Ar}$), 130.6 ($C_{Ar}$), 134.2 ($C_{Ar}$), 134.6 (C–Cl), 135.1 (CH=C), 137.9 (Ar–CH), 189.8 (C=O). MS/MS (*m/z*): $[M^+H]^+$ cald. 343.0651 found 343.0658.

**Synthesis of 3,5-bis((*E*)-2-chlorobenzylidene)piperidin-4-one (4).** Compound **4** was synthesized according to the previous method [10]. The 2-chlorobenzaldehyde (0.45 mL, 4 mmol), 4-piperidone monohydrate hydrochloride (0.3 g, 2 mmol), and ethanol (20 mL) were initially mixed and stirred at 65 °C for 15 min. Then, hydrochloric acid 37% was added and the mixture was stirred at 65 °C for 96 h. The resulting precipitate was filtered, washed with distilled water and recrystallized from hot methanol. Yellow solid; yield: 44%; purity: 100%; m.p.: 211.0–212.7 °C; FTIR (cm$^{-1}$): 3425 (N–H), 2916 ($C_{sp^3}$–H), 1682 (C=O), 1435 (Ar C=C), 1188 (C-N), 732 (C–Cl); $^1$H-NMR (DMSO-$d_6$, 500 MHz) δ (ppm): 4.32 (*s*, 4H, $CH_2$), 7.47 (*m*, 6H, $H_{Ar}$), 7.62 (*m*, 2H, $H_{Ar}$), 7.96 (*s*, 2H, CH=C), 9.76 (*s*, 1H, NH). $^{13}$C-NMR (DMSO-$d_6$, 125 MHz) δ (ppm): 44.3 ($CH_2$), 128.1 ($C_{Ar}$), 130.3 ($C_{Ar}$), 130.5 ($C_{Ar}$), 131.3 ($C_{Ar}$), 132.2 ($C_{Ar}$), 132.3 (C–Cl), 134.6 (CH=C), 136.4 (Ar–CH), 182.8 (C=O). MS/MS (*m/z*): $[M^+H]^+$ cald. 344.0603 found 344.0605.

**Synthesis of 1-benzyl-3,5-bis((*E*)-2-chlorobenzylidene)piperidin-4-one (6).** Compound **6** was prepared by following the procedure as described for curcumin analogue **3**. The mixture of 2-chlorobenzaldehyde (0.45 mL, 4 mmol), *N*-benzyl-4-piperidone (0.38 mL, 2 mmol), ethanol (10 mL), and sodium hydroxide (40%, 3 mL) was stirred at room temperature for 3 h. Yellow solid; yield: 71%; purity: 96%, m.p.: 160–162 °C; FTIR (cm$^{-1}$): 2937 ($C_{sp^3}$–H), 1669 (C=O), 1456 (Ar C=C), 1191 (C–N), 751 (C–Cl); $^1$H-NMR ($CDCl_3$, 500 MHz) δ (ppm): 3.60 (*s*, 2H, $CH_2$), 3.72 (*s*, 4H, $CH_2$), 7.09 (*d*, *J* = 8 Hz, 1H, $H_{Ar}$), 7.17 (*m*, 8H, $H_{Ar}$), 7.24 (*t*, *J* = 8 Hz, 2H, $H_{Ar}$), 7.42 (*d*, *J* = 8 Hz, 2H, $H_{Ar}$), 7.99 (*s*, 2H, CH=C); $^{13}$C-NMR ($CDCl_3$, 125 MHz) δ (ppm): 53.6 ($CH_2$), 60.2 ($CH_2$), 126.4 ($C_{Ar}$), 127.4 ($C_{Ar}$), 128.3 ($C_{Ar}$), 128.9 ($C_{Ar}$), 129.1 ($C_{Ar}$), 129.9 ($C_{Ar}$), 130.0

($C_{Ar}$), 130.3 ($C_{Ar}$), 133.7 (C–Ar), 134.6 (C–Cl), 135.1 (CH=C), 137.3 (Ar–CH), 187.3 (C=O). MS/MS (*m/z*): $[M^+H]^+$ cald. 434.1073 found 434.1073.

### In vitro *antiplasmodium assay of curcumin analogous*

The antiplasmodium assay was performed against chloroquine-sensitive (3D7) and chloroquine-resistant (FCR3) *P. falciparum* according to the method of Rieckmann et al. [15] with slight modifications [16]. Each compound was dissolved in DMSO and RPMI medium to get the final concentrations of 10.00, 5.00, 2.50, 1.25 and 0.625 μg/mL. Next, as much as 100 μL of the testing compound in various concentrations was subjected to the 96-well microplate and 100 μL of parasite suspension was then added. Each series of concentrations was replicated three times. The microplate was incubated at 37 °C for 72 h. Subsequently, a thin blood smear was made using 20% Giemsa stain. Finally, the percentage of parasitemia and the inhibition percentage of *P. falciparum* growth were counted from the number of erythrocytes for every 1,000 erythrocytes using a microscope with 1,000 magnifications. The $IC_{50}$ value was determined by the probit analysis using SPSS statistics 26 software.

### *Prediction of the ADMET parameters of curcumin analogous*

The physicochemical and pharmacokinetic (ADMET) parameters were predicted using the online webserver ADMETlab 2.0 (https://admetmesh.scbdd.com/) [17], pkCSM (https://biosig.lab.uq.edu.au/pkcsm/prediction) [18] and admetSAR (http://lmmd.ecust.edu.cn/admetsar2) [19] by entering the SMILES list of curcumin analogous.

## ■ RESULTS AND DISCUSSION

### Molecular Docking Study of Curcumin Analogous

Molecular docking is one of the widely used tools in computer-aided drug design. It is used to determine the interaction between drugs and target proteins. In this study, P*f*ENR, P*f*LDH, and P*f*ATP6 were chosen as target receptors since they played important roles in various metabolic and biochemical pathways of the *Plasmodium* parasite [12]. The validation of molecular docking was conducted by redocking the proteins with their native ligands. The validation parameter used was root mean square deviation (RMSD). The RMSD value which was less than 2 Å indicated the accuracy of the docking program [20]. The results demonstrated that all target receptors had RMSD less than 2 Å. The results of molecular docking of six curcumin analogous and curcumin as comparing ligands to the corresponding three receptor targets were shown in Table 1.

The docking study revealed that all the tested curcumin analogous **1**-**6** had a lower binding affinity for the three target receptors than the native ligands and curcumin, indicating that they created more stable interactions with P*f*ENR, P*f*LDH, and P*f*ATP6 targets than the native ligands and curcumin. Additionally, all analogous also specifically interacted with key residues of each receptor target.

Silva et al. [21] and Tallorin et al. [22] reported that π-π interaction with Tyr267 or Tyr277 and the hydrogen interaction with Tyr277 were significant for the binding to the active sites of P*f*ENR. In this case, the analogous **1**-**3** formed the π-π stacked interaction with Tyr267, while **5** and **6** showed π-π T shaped interaction with Tyr267. On the other hand, analogue **4** formed hydrogen bonding to Tyr277 (Table 1).

Lactate dehydrogenase (P*f*LDH) had active sites at Ala98, Ile54, Glu122, Ile119, Phe52, and Val26 [23]. All analogous inhibited the action of lactate dehydrogenase through the interactions with the amino acid residues of Ala98, Ile54, Ile119, Phe52, and Val26 *via* alkyl/π-alkyl and π-σ interaction. The analogue **4** had the hydrogen bond interaction that occurred between Glu122 and the hydrogen atom in the amine group. The analogue **6** also interacted with Glu122 *via* the hydrogen bond (Table 1).

The active site residues of P*f*ATP6 consisted of Leu263, Phe264, Gln267, Ile977, Ile981, Ala985, Asn1039, Leu1040, Ile1041, and Asn1042 [24]. Curcumin has been reported as a potential inhibitor of P*f*ATP6 [25]. Curcumin bonded to P*f*ATP6 *via* two hydrogen bonds with Ile1041 and Asn1039 residues and *via* alkyl/π-alkyl interaction with Ile977, Ile981, Ile272, Ile275, Ala313, Val984, Ile1041 and Leu1046. Compared to these interactions, curcumin analogous **1**-**6** also had alkyl/π-alkyl interaction with almost all these amino acids. In addition, only curcumin analogue **4** had hydrogen bond

**Table 1.** Molecular docking of curcumin analogous **1**-**6** with P*f*ENR, P*f*LDH, and P*f*ATP6

| Receptor targets | Ligands | Binding affinity (kcal/mol) | Interactions |
|---|---|---|---|
| P*f*ENR | TCL (Native ligand) | −6.13 | H-bond: Tyr277<br>Alkyl/π-alkyl: Ala219, Ala217, Ala319, Ala320, Ile369, Pro314, Phe368, Ala327, Val222, Met281<br>π-π T shaped: Tyr267<br>van der Waals: Ile323, Lys285, Asn218 |
| | 1 | −8.31 | H-bond: Lys285<br>Alkyl/π-alkyl: Tyr267, Pro314, Ala312, Ala319, Ala217, Ala219, Val222<br>π-π stacked: Tyr267<br>van der Waals: Tyr111, Gly313, Leu315, Ile323, Tyr277, Asn218 |
| | 2 | −8.71 | H-bond: Lys285<br>Alkyl/π-alkyl: Tyr267, Ala219, Val222, Ala217, Ala319, Pro314, Ala312, Tyr277, Met281<br>π-π stacked: Tyr267<br>van der Waals: Tyr111, Gly313, Leu315, Ala320, Ile323, Asn218 |
| | 3 | −9.32 | H-bond (C): Tyr277<br>Alkyl/π-alkyl: Tyr267, Pro314, Ala320, Ile323, Ala319, Ala219, Met281, Val222, Ala217<br>π-π T shaped: Tyr267<br>van der Waals: Tyr111, Gly313, Leu315, Asn218, Ala312, Tyr277 |
| | 4 | −8.83 | H-bond: Tyr277<br>Alkyl/π-alkyl: Ile369, Ala372, Pro314, Ile323, Ala319, Ala322, Ala217, Ala219, Met281, Val222<br>van der Waals: Asn218 Lys285, Tyr267, Gly313, Leu315, Tyr111, Ala320, Ser317 |
| | 5 | −7.79 | Alkyl/π-alkyl: Pro314, Ile323, Ile369, Ala320, Ala319<br>π-π T shaped: Tyr267<br>van der Waals: Lys285, Gly313, Leu265, Arg318, Gly104, Ser215, Gly112, Gly110, Ser317, Tyr111, Leu315, Tyr277 |
| | 6 | −10.03 | H-bond: Tyr277<br>Alkyl/π-alkyl: Ala320, Pro314, Ala319, Ile323, Val222, Ala322, Leu265, Ala312<br>π-π T shaped/stacked: Tyr267, Tyr111<br>van der Waals: Thr266, Lys285, Met281, Ala217 Asn218, Tyr277, Leu315, Gly313 |
| | Curcumin | −7.74 | H-bond: Thr266, Gly313<br>H-bond (C): Ala312, Pro314, Gly313<br>Alkyl/π-alkyl: Ala320, Tyr267, Pro314<br>π-σ: Tyr267<br>van der Waals: Leu265, Ser311, Ile310, Ala217, Ala218, Met281, Ala319, Ile323, Leu315, Ser317, Tyr277, Tyr111 |
| P*f*LDH | CLQ (Native ligand) | −6.32 | H-bond: Glu122<br>Alkyl/π-alkyl: Ala98, Ile119, Phe52, Val26<br>π-σ: Ile54, Ile119<br>Salt bridge: Glu122 |

| Receptor targets | Ligands | Binding affinity (kcal/mol) | Interactions |
|---|---|---|---|
| | | | van der Waals: Phe100, Gly27, Ile123, Tyr85, Lys118 |
| | 1 | −6.86 | Alkyl/π-alkyl: Ala98, Ile54, Val26, Lys118<br>π-σ: Lys118, Ala98<br>van der Waals: Phe100, Gly27, Asp53, Ile123, Phe52, Tyr85, Lys119, Glu122 |
| | 2 | −7.52 | Alkyl/π-alkyl: Ala98, Ile54, Ile119, Lys118<br>π-σ: Lys118, Ala98<br>van der Waals: Phe100, Gly99, Ser28, Gly27, Phe52, Tyr85, Val26, Glu122 |
| | 3 | −8.16 | H-bond (C): Ile119<br>Alkyl/π-alkyl: Ala98, Ile54, Ile119, Lys118, Leu115<br>π-σ: Ala98, Ile54<br>van der Waals: Phe100, Tyr85, Glu122, Phe52, Gly99, Gly27, Asp53, Val26, Phe52, Ile123 |
| | 4 | −9.14 | H-bond: Glu122<br>Alkyl/π-alkyl: Ala98, Ile54, Ile119, Val26, Lys118, Phe100, Leu115<br>π-σ: Ala98<br>van der Waals: Gly99, Gly27, Asp53, Phe52, Tyr85, Ile123 |
| | 5 | −8.40 | Alkyl/π-alkyl: Ala98, Ile54, Ile119, Lys118, Val26<br>π-σ: Ala98<br>van der Waals: Phe100, Gly99, Asp53, Gly27, Phe52, Tyr85, Glu122, Ile123 |
| | 6 | −9.19 | H-bond (C): Glu122<br>Alkyl/π-alkyl: Ile54, Ile119, Val26, Lys118<br>π-σ: Ala98, Ile54, Phe100<br>van der Waals: Gly27, Phe52, Ile123, Asp53, Tyr85, Val55, Gly99 |
| | Curcumin | −6.78 | H-bond: Gly99<br>H-bond (C): Glu122, Asp53<br>Alkyl/π-alkyl: Ile119, Ala98<br>π-π T shaped: Phe100<br>van der Waals: Gly27, Ile54, Thr101, Val26, Phe52, Ile123, Tyr85, Lys118 |
| P*f*ATP6 | 1 | −8.91 | Alkyl/π-alkyl: Ile271, Leu263, Ile977, Phe264, Lys260, Leu1046, Leu1040<br>π-π T shaped: Phe264<br>π-σ: Leu268<br>van der Waals: Gln267, Ile1041, Tyr1049, Ile981, Asn1039 |
| | 2 | −8.43 | Alkyl/π-alkyl: Val984, Ile272, Ala313, Ile275, Ile981, Phe988<br>π-σ: Ala985, Val984, Ile981<br>van der Waals: Ile271, Ile977, Leu268, Asn980, Thr1054, Ile989 |
| | 3 | −9.69 | Alkyl/π-alkyl: Tyr1049, Ile977, Ile271, Ile1041, Phe264, Lys260, Leu268, Leu1040, Leu1046<br>van der Waals: Leu263, Gln267, Asn1039, Ile981 |
| | 4 | −9.06 | H-bond: Ile1041<br>Alkyl/π-alkyl: Ile271, Ile1041, Phe264, Lys260, Leu1046, Leu1040<br>van der Waals: Leu263, Gln267, Asn1039, Ile981, Ile977, Tyr1049 |
| | 5 | −8.79 | Alkyl/π-alkyl: Tyr1049, Ile977, Leu268, Ile272, Phe264, Ile981, Ala313, Val984, Ile1041, Leu1046<br>van der Waals: Pro315, Asn980, Ile271, Ile275, Gln267 |

| Receptor targets | Ligands | Binding affinity (kcal/mol) | Interactions |
|---|---|---|---|
| | 6 | −10.49 | Alkyl/π-alkyl: Ala985, Ile275, Ile271, Ile272, Ile981, Ala313, Leu268, Ile977, Leu1046, Tyr1049<br>π-σ: Val984<br>van der Waals: Phe988, Ile1050, Phe264, Pro315, Thr1054, Asn980 |
| | Curcumin | −7.94 | H-bond: Ile1041, Asn1039<br>Alkyl/π-alkyl: Ile977, Ile981, Ile272, Ile275, Ala313, Val984, Ile1041, Leu1046<br>van der Waals: Gln267, Phe264, Leu268, Ile271, Asn980, Tyr1049, Leu1040, Asn1042 |

interaction with Ile 1041 as in curcumin. Moreover, Dohutia et al. [14] reported that interaction π-σ or π-alkyl with Leu268 could increase antimalarial activity. Based on the molecular docking study, curcumin analogues **3** and **6** were found to bind Leu268 *via* π-alkyl interaction, while curcumin analogue **1** had π-σ interaction with Leu268.

The selection of three curcumin analogues as antimalarial candidates was carried out by considering the low binding affinity and the resulting interactions with amino acid residues on the active sites of the three target receptors. The docking study revealed that curcumin analogous **3**, **4**, and **6** displayed better antimalarial activity against P*f*ENR, P*f*LDH, and P*f*ATP6 than other analogues. Thus, curcumin analogous **3**, **4**, and **6** were recommended to be synthesized. The visualization of the interaction between curcumin analogous **3**, **4**, and **6** was presented in Fig. 2.

## Synthesis of Curcumin Analogous

Synthesis of curcumin analogous **3**, **4**, and **6** was carried out *via* aldol condensation (Fig. 3). Compounds **3** and **6** were prepared by reacting 2-chlorobenzaldehyde with cyclohexanone and *N*-benzyl-4-piperidone in the presence of a NaOH catalyst. On the other hand, compound **4** was obtained from 2-chlorobenzaldehyde and 4-piperidone *via* an aldol condensation reaction using a hydrochloric acid catalyst. The results showed that the curcumin analogous could be obtained in good yields.

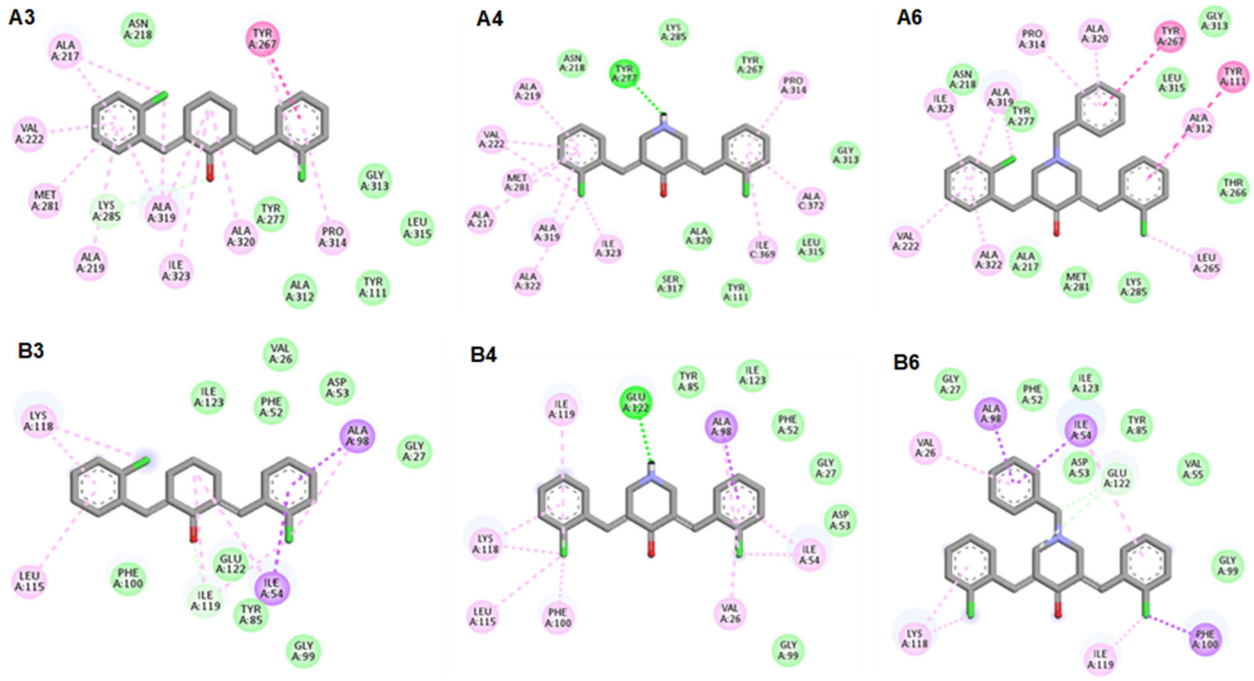

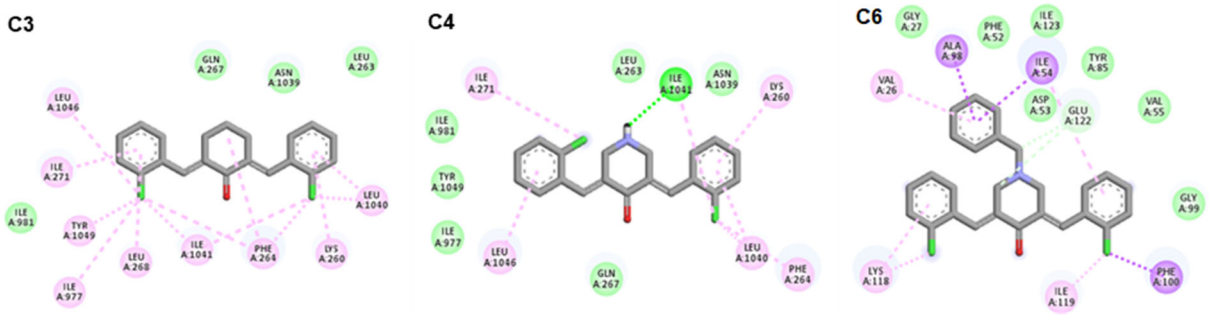


**Fig 2.** Visualization of the interaction of **3**, **4**, and **6** compounds on (A) P*f*ENR; (B) P*f*LDH, and (C) P*f*ATP6

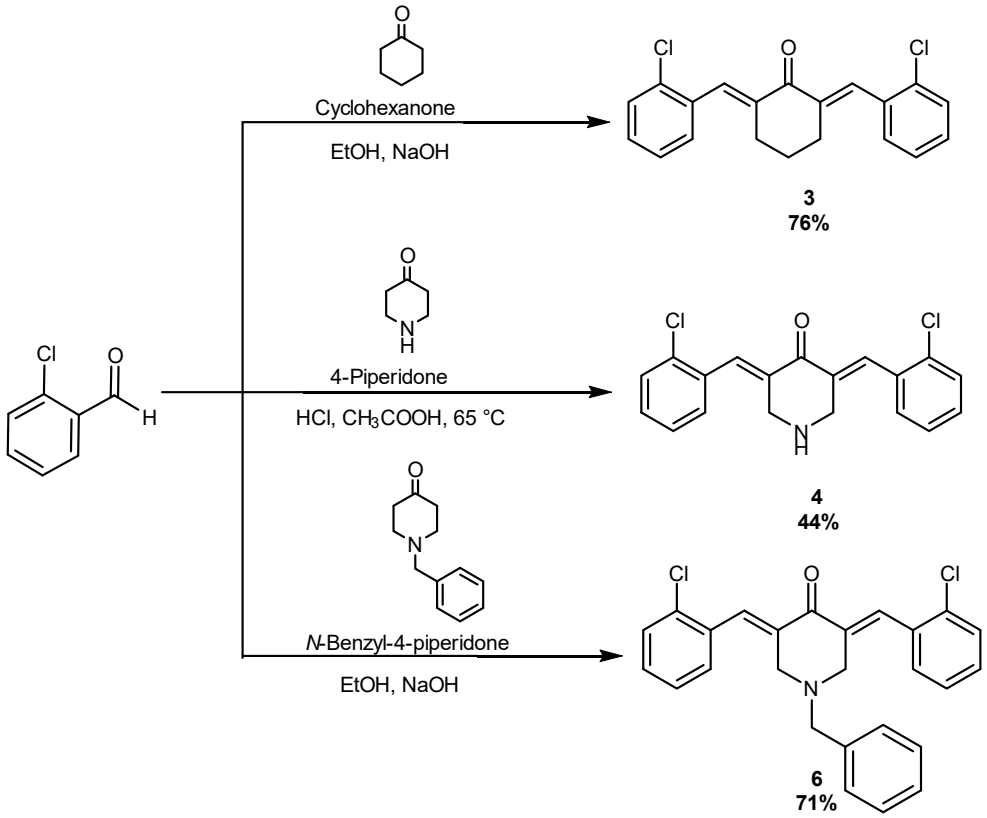


**Fig 3.** Synthesis of curcumin analogous (**3**), (**4**) and (**6**)

According to NMR analysis, the formation of monoketone curcumin was confirmed by the presence of one singlet at 7.90–7.99 ppm representing the alkene proton. Additionally, the alkene carbons (Cα and Cβ) of curcumin analogous resonated in the region of 134–138 ppm. The FTIR spectra also affirmed the formation of curcumin analogous by the appearance of absorption bands at 1668 $cm^{-1}$ representing the conjugated C=O group. The peak at 732 and 751 $cm^{-1}$ corresponded to the C–Cl stretching. In addition, compounds **4** and **6** demonstrated the absorption bands at 1188 and 1191 $cm^{-1}$ corresponding to C–N aliphatic stretching. The mass spectrum of curcumin analogous **3**, **4**, and **6** showed that molecular ions $[M^+H]^+$ at *m/z* 343.0658, 344.0605, and 434.1073 were in line with the calculated mass.

### *In Vitro* Antiplasmodium Assay of Curcumin Analogous

The *in vitro* antiplasmodium assay of the synthesized curcumin analogous **3**, **4**, and **6** as well as curcumin, was tested against FCR3 and 3D7 *P.*

*falciparum*. The tested compounds can be considered to show potent antimalarial activity if they have an $IC_{50}$ value less than 1 μM; good activity, if the $IC_{50}$ value is between 1–20 μM; moderate activity, if the $IC_{50}$ value is between 20–100 μM; low activity; if the $IC_{50}$ value is between 100–200 μM and not active if the $IC_{50}$ value is greater than 200 μM [26]. The antiplasmodium evaluation against FCR3 strain showed that analogue **6** had potent activity, while compounds **3** and **4** showed good activity (Table 2). Compounds **3**, **4**, and **6** displayed good activity against 3D7 strain (Table 2). In addition, the $IC_{50}$ values of compounds **3**, **4**, and **6** were lower than that of curcumin for both *P. falciparum* strains demonstrating that all curcumin analogous **3**, **4**, and **6** were more active than curcumin.

The antiplasmodium potencies of the curcumin analogous against *P. falciparum* 3D7 were compared with other analogous synthesized in the previous works [8,27-28]. The effect of chloro substituent position in the aromatic ring showed that the placement of chloro

**Table 2.** $IC_{50}$ values and resistance index of curcumin analogous **3**, **4**, and **6**

| Entry | Compound | $IC_{50}$ (μM) | | Resistance Index ($IC_{50}^{FCR3}/IC_{50}^{3D7}$) |
|---|---|---|---|---|
| | | FCR3 | 3D7 | |
| 1 | 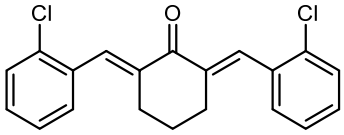 (**3**) | 1.07 | 2.41 | 0.44 |
| 2 | 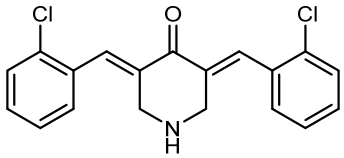 (**4**) | 2.58 | 3.06 | 0.84 |
| 3 | 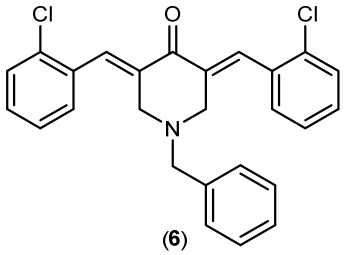 (**6**) | 0.76 | 1.09 | 0.70 |
| 4 | 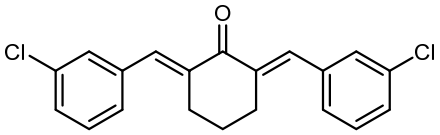 (**7**) | _ | 3.00 [27] | _ |
| 5 | 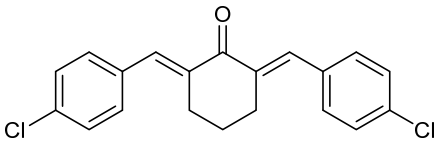 (**8**) | _ | 8.50 [27] | _ |
| 6 | 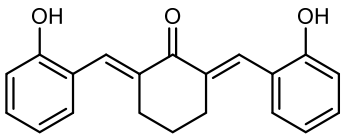 (**9**) | _ | 11.5 [28] | _ |

| Entry | Compound | $IC_{50}$ (μM) | | Resistance Index ($IC_{50}^{FCR3}/IC_{50}^{3D7}$) |
|---|---|---|---|---|
| | | FCR3 | 3D7 | |
| 7 | 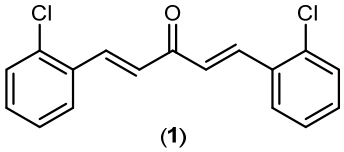 (**1**) | _ | 6.26 [8] | _ |
| 8 | 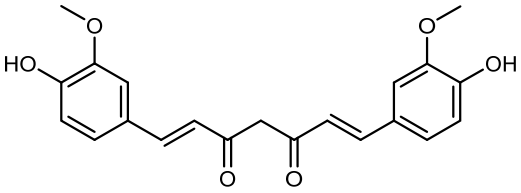 Curcumin | 8.79 | 9.17 | 0.96 |

substituent at the 2- and 3- positions might enhance the antiplasmodium activities (Table 2, entry 1 vs 4 and 5). It should be noted that the electron-withdrawing effect from the chloro group gave higher activity than the hydroxyl group as an electron-donating group (Table 2, entry 1 vs 6). In addition, higher activities were observed when six-membered rings were installed in curcumin analogous (Table 2, entries 1, 2, and 3 vs 7). Therefore, the presence of chloro substituent in the 2 position and six-membered rings might be responsible for the higher antiplasmodium activities of curcumin analogous.

Salas et al. [29] stated that the resistance index (RI) was a valuable tool for the analysis of antiplasmodium candidates. The resistance index could be determined as the ratio of the $IC_{50}$ of the resistant strain to that of the sensitive strain. The large RI value indicated the higher resistance level of the tested compounds. On the contrary, the small RI value indicated that the tested compounds were not susceptible to resistance and had the potential to develop as drug candidates. The RI values for all analogous were smaller than curcumin (Table 2) and the reference drug of chloroquine with the range of RI values of 11–14 [16,30]. From the evaluation of $IC_{50}$ and RI values, it can be concluded that curcumin analogous **3**, **4**, and **6** had great potential as antiplasmodium candidates.

## Prediction of ADMET Parameters of Curcumin Analogous

The *in silico* prediction of ADMET parameters for all curcumin analogous and curcumin was depicted in Table 3. The physicochemical parameters of the analogous were analyzed on the basis of Lipinski's Rule of Five. According to Table 3, the molecular weight of the analogous **3**, **4**, and **6** ranged from 343.25 to 434.36 g/mol, the amount of HBA ranged from 1 to 2, the amount of HBD ranged from 0 to 1 and the log P value ranged from 4.33 to 5.66. While the curcumin analogue **4** met the Lipinski Rules of Five, the analogues **3** and **4** violated one parameter of log P. Chander et al. [31] also stated that 95% of clinically approved drugs had the following range of physicochemical properties: molecular weight (130–725), HA (2–20), HD (0–6) and log P (−2 to 6.5). Therefore, all the analogous **3**, **4**, and **6** met the physicochemical properties as stated in the previous study [31]. In addition, it could be predicted that the analogous **3**, **4**, and **6** would be easily absorbed and had high permeability.

Caco-2 permeability, human intestinal absorption (HIA) and skin permeability were used to predict the absorption level of the curcumin analogous (Table 3). A compound will be considered to have a high Caco-2 permeability if it has $\log P_{app} > 0.90$ cm/s [18]. All analogous were predicted to have high Caco-2 permeability and curcumin, however, had low Caco-2 permeability. In the case of human intestinal absorption, an absorption value of higher than 80% is considered to be well absorbed [31]. As expected, all analogous had better HIA values and good absorption than curcumin. A molecule will be considered to have excellent skin permeability if the permeability coefficient (Papp) is more than $2 \times 10^{-6}$ cm/s [17]. The prediction showed that all curcumin analogous had good skin permeability.

**Table 3.** Prediction of physicochemical and ADMET parameters

| Parameters | Compound | | | |
|---|---|---|---|---|
| | **3** | **4** | **6** | Curcumin |
| Lipinski's rule | | | | |
| Molecular weight <500Da | 343.250 | 344.230 | 433.360 | 368.380 |
| nHBA <10 | 1 | 2 | 2 | 6 |
| nHBD <5 | 0 | 1 | 0 | 2 |
| log P <5 | 5.437 | 4.330 | 5.664 | 2.740 |
| (A) Absorption | | | | |
| Caco-2 permeability (log cm/s) | 1.604 | 1.576 | 1.089 | 0.093 |
| Human intestinal absorption (HIA) (%) | 93.589 | 90.323 | 90.365 | 82.190 |
| Skin permeability (cm/s) | $8.0 \times 10^{-6}$ | $9.0 \times 10^{-6}$ | $1.1 \times 10^{-5}$ | $1.6 \times 10^{-5}$ |
| (D) Distribution | | | | |
| Volume distribution (L/kg) | 0.392 | 0.717 | 0.546 | 0.369 |
| BBB (log BB) | 0.025 | 0.766 | 0.215 | 0.103 |
| (M) Metabolism | | | | |
| CYP2D6 substrate | No | No | No | Yes |
| CYP3A4 substrate | No | No | Yes | Yes |
| CYP1A2 substrate | No | Yes | Yes | Yes |
| CYP2C19 substrate | No | No | No | No |
| CYP2C9 substrate | No | No | No | Yes |
| CYP2D6 inhibition | No | Yes | Yes | No |
| CYP3A4 inhibition | No | No | No | Yes |
| CYP1A2 inhibition | Yes | Yes | No | Yes |
| CYP2A19 inhibition | Yes | Yes | Yes | Yes |
| CYP2C9 inhibition | Yes | No | Yes | Yes |
| (E) Excretion | | | | |
| Clearance (mL/min/kg) | 5.504 | 7.127 | 9.993 | 13.839 |
| (T) Toxicity | | | | |
| Rat oral acute toxicity (mol/kg) | 2.764 | 3.006 | 2.775 | 1.833 |
| Ames toxicity | No | No | Yes | No |
| Hepatotoxicity | No | Yes | No | No |

The distribution volume (VD) and the blood-brain barrier membrane permeability (log BB) were used to describe the distribution of a compound. The distribution volume is a parameter to calculate the volume in which the whole quantity of a drug will be circulated at an equal level of blood plasma. A compound will be assumed to have a proper VD if it has a VD value in the range of 0.04–20.00 L/kg [17]. According to Table 3, the volume of distribution of all curcumin analogous was categorized as good. The blood-brain barrier (BBB) is a parameter to determine the ability of a medicine to pass through the brain. This parameter is important in regard to decreasing the side effects and toxicity of drugs. When log BB is higher than 0.3, a compound would easily cross the blood-brain barrier. However, a compound would hardly reach the brain when the log BB value is lower than −1. The analogue **4** was predicted to easily cross the blood-brain barrier, whereas the analogous **3** and **6** might moderately penetrate the blood-brain barrier.

Cytochrome P450 is an essential enzyme for the detoxification of foreign chemicals and the metabolism of drugs. There are five CYP450 enzymes that metabolize 90% of the drugs, namely CYP1A2, CYP2C9, CYP2C19, CYP2D6, and CYP3A4 [32]. As displayed in Table 3, analogue **3** was not the substrate for all CYP450 enzymes, analogue **4** was the substrate for CYP1A2 and

analogue **6** was the substrate for CYP1A2 and CYP3A4. Additionally, analogue **3** was predicted to inhibit CYP1A2, CYP2C19, and CYP2C9, analogue **4** was predicted to inhibit CYP2D6, CYP1A2 and CYP2C19 and analogue **6** was predicted to inhibit CYP2D6, CYP2C19 and CYP2C9. The prediction suggested that analogous **4** and **6** may be metabolized in the liver. Curcumin might act as both a substrate and inhibitor of most CYP450 enzymes, indicating that curcumin might be metabolized in the liver.

The excretion parameter was evaluated by predicting the clearance rate (Cl). The higher the Cl value of a compound, the faster the compound is removed from the body. The prediction showed that the total clearance of curcumin was higher than curcumin analogous **3**, **4**, and **6**, indicating that the analogous had slower elimination in the body (Table 3).

The potential toxicity of a compound might be predicted based on acute oral toxicity ($LD_{50}$), Ames toxicity, and hepatotoxicity. From Table 3, all curcumin analogs had $LD_{50}$ values ranging from 2.764 to 3.006 mol/kg, which seems to be sufficiently safe [33]. The Ames assay is a method used to predict the mutagenic potential of a compound. In this context, analogue **6** was predicted to have a mutagenic effect. Hepatotoxicity is a test performed to predict chemicals that might induce liver damage. The prediction indicated that only analogue **4** might induce the hepatotoxic effect. Therefore, the modification of the curcumin structure by replacing the β-diketone group with a monoketone and by introducing chloro substitution at the 2-position could increase the bioavailability of curcumin.

## ■ CONCLUSION

The molecular docking study showed that the curcumin analogous **3**, **4**, and **6** had low binding affinity and specific interactions with amino acid residues in the receptor targets of P*f*ENR, P*f*LDH, and P*f*ATP6. The analogous **3**, **4**, and **6** were successfully synthesized from 2-chlorobenzaldehyde and various ketones in good yields. The modification of curcumin by replacing the β-diketone group with a monoketone and by introducing both chloro substitutions at the 2-position and six-membered ring into the structure of analogous could improve the pharmaceutical properties of curcumin as antiplasmodium, including the increase the *in vitro* activity against *P. falciparum* 3D7 and FCR3 strains, the decrease of RI value and the enhancement of ADMET profiles. Our study showed that the curcumin analogous **3**, **4**, and **6** had great potential to be antiplasmodium candidates. Further study is required to carry out molecular dynamics simulations to observe the stability of the protein and ligand complex interactions.

## ■ ACKNOWLEDGMENTS

The financial support from Dr. Muhammad Idham Darussalam Mardjan S.Si., M.Sc. (Universitas Gadjah Mada) is highly acknowledged. The authors would also like to thank Prof. Laurent Commeiras (Aix-Marseille Université) for the fine-tuning of the manuscript.

## ■ AUTHOR CONTRIBUTIONS

Chessy Rima Mustika performed the molecular docking, synthesis, antiplasmodium assay and ADMET prediction, as well as the preparation of the manuscript. Endang Astuti conducted the conceptualization, writing-review, and supervision. Muhammad Idham Darussalam Mardjan contributed to writing-review, editing and supervision.

## ■ REFERENCES

[1] Snow, R.W., 2015, Global malaria eradication and the importance of *Plasmodium falciparum* epidemiology in Africa, *BMC Med.*, 1 (13), 23.

[2] Antony, H.A., and Parija, S.C., 2016, Antimalarial drug resistance: An overview, *Trop. Parasitol.*, 6 (1), 30–41.

[3] Theppawong, A., Kaur, G., Kumar, V., Van Camp, J., and D'hooghe, M., 2020, Synthetic strategies in curcumin chemistry focused on anticancer applications, *ARKIVOC*, 7, 257–305.

[4] Rasmussen, H.B., Christensen, S.B., Kvist, L.P., and Karazmi, A., 2000, A simple and efficient separation of the curcumins, the antiprotozoal constituents of *Curcuma longa*, *Planta Med.*, 66 (4), 396–398.

[5] Kunnumakkara, A.B., Bordoloi, D., Padmavathi, G., Monisha, J., Roy, N.K., Prasad, S., and Aggarwal,

B.B., 2017, Curcumin, the golden nutraceutical: Multitargeting for multiple chronic diseases, *Br. J. Pharmacol.*, 174 (11), 1325–1348.

[6] Shetty, D., Kim, Y.J., Shim, H., and Snyder, J.P., 2015, Eliminating the heart from the curcumin molecule: Monocarbonyl curcumin mimics (MACs), *Molecules*, 20 (1), 249–292.

[7] Yin, S., Zheng, X., Yao, X., Wang, Y., and Liao, D., 2013, Synthesis and anticancer activity of mono-carbonyl analogues of curcumin, *J. Cancer Ther.*, 4 (1), 113–123.

[8] Aher, R.B., Wanare, G., Kawathekar, N., Kumar, R.R., Kaushik, N.K., Sahal, D., and Chauhan, V.S., 2011, Dibenzylideneacetone analogues as novel *Plasmodium falciparum* inhibitors, *Bioorg. Med. Chem. Lett.*, 10 (21), 3034–3036.

[9] Eryanti, Y., Hendra, R., Herlina, T., Zamri, A., and Supratman, U., 2018, Synthesis of *N*-methyl-4-piperidone curcumin analogues and their cytotoxicity activity against T47D cell lines, *Indones. J. Chem.*, 18 (2), 362–366.

[10] Damayanti, P.N., Ritmaleni, R., and Setyowati, E.P., 2020, Synthesis and antibacterial activity of 4-piperidone curcumin analogues against Gram-positive and Gram-negative bacteria, *Res. J. Pharm. Technol.*, 13 (10), 4765–4769.

[11] Ekawati, L., Purwono, B., and Mardjan, M.I.D., 2020, Synthesis *N*-phenyl pyrazoline from dibenzalacetone and heme polymeration inhibitory activity (HPIA) assay, *Key Eng. Mater.*, 840, 245–250.

[12] Kumar, S., Bhardwaj, T.R., Prasad, D.N., and Singh, R.K., 2018, Drug targets for resistant malaria: Historic to future perspectives, *Biomed. Pharmacother.*, 104, 8–27.

[13] Han, D., Su, M., Tan, J., Li, C., Zhang, X., and Wang, C., 2016, Structure–activity relationship and binding mode studies for a series of diketo-acids as HIV integrase inhibitors by 3D-QSAR, molecular docking and molecular dynamics simulations, *RSC Adv.*, 6 (33), 27594–27606.

[14] Dohutia, C., Chetia, D., Gogoi, K., and Sarma, K., 2017, Design, *in silico* and *in vitro* evaluation of curcumin analogues against *Plasmodium falciparum*, *Exp. Parasitol.*, 175, 51–58.

[15] Rieckmann, K.H., Campbell, G.H., Sax, L.J., and Ema, J.E., 1978, Drug sensitivity of *Plasmodium falciparum*: An *in-vitro* microtechnique, *Lancet*, 311 (8054), 22–23.

[16] Zakiah, M., Syarif, R.A., Mustofa, M., Jumina, J., Fatmasari, N., and Sholikhah, E.N., 2021, *In vitro* antiplasmodial, heme polymerization, and cytotoxicity of hydroxyxanthone derivatives, *J. Trop. Med.*, 2021, 8866681.

[17] Xiong, G., Wu, Z., Yi, J., Fu, L., Yang, Z., Hsieh, C., Yin, M., Zeng, X., Wu, C., Lu, A., Chen, X., Hou, T., and Cao, D., 2021, ADMETlab 2.0: An integrated online platform for accurate and comprehensive predictions of ADMET properties, *Nucleic Acids Res.*, 49 (W1), W5–W14.

[18] Pires, D.E.V., Blundell, T.L., and Ascher, D.B., 2015, pkCSM: Predicting small-molecule pharmacokinetic and toxicity properties using graph-based signatures, *J. Med. Chem.*, 58 (9), 4066–4072.

[19] Yang, H., Lou, C., Sun, L., Li, J., Cai, Y., Wang, Z., Li, W., Liu, G., and Tang, Y., 2019, admetSAR 2.0: Web-service for prediction and optimization of chemical ADMET properties, *Bioinformatics*, 35 (6), 1067–1069.

[20] Ramírez, D., and Caballero, J., 2018, Is it reliable to take the molecular docking top scoring position as the best solution without considering available structural data?, *Molecules*, 23 (5), 1038.

[21] Silva, D.A.A., da Costa, D.M., Oliveira, L.M., Brandão, H.N., Alves, C.Q., Santos Jr., A.F., and dos Santos Jr., M.C., 2020, Identification of flavonoids as inhibitors of *Plasmodium falciparum* enoyl-ACP reductase by hierarchical virtual screening, *J. Braz. Chem. Soc.*, 31 (12), 2544–2552.

[22] Tallorin, L., Durrant, J.D., Nguyen, Q.G., McCammon, J.A., and Burkart, M.D., 2014, Celastrol inhibits *Plasmodium falciparum* enoyl-acyl carrier protein reductase, *Bioorganic Med. Chem.*, 22 (21), 6053–6061.

[23] Zakaria, N.H., Wai, L.K., and Hassan, N.I., 2020,

Molecular docking study of the interactions between *Plasmodium falciparum* lactate dehydrogenase and 4-aminoquinoline hybrids, *Sains Malays.*, 49 (8), 1905–1913.

[24] Nagasundaram, N., George Priya Doss, C., Chakraborty, C., Karthick, V., Thirumal Kumar, D., Balaji, V., Siva, R., Lu, A., Ge, Z., and Zhu, H., 2016, Mechanism of artemisinin resistance for malaria P*f*ATP6 L263 mutations and discovering potential antimalarials: An integrated computational approach, *Sci. Rep.*, 6 (1), 30106.

[25] Ji, H.F., and Shen, L., 2009, Interactions of curcumin with the P*f*ATP6 model and the implications for its antimalarial mechanism, *Bioorg. Med. Chem. Lett.*, 19 (9), 2453–2455.

[26] Batista, R., De Jesus Silva Junior, A., and De Oliveira, A.B., 2009, Plant-derived antimalarial agents: new leads and efficient phytomedicines. Part II. Non-alkaloidal natural products, *Molecules*, 14 (8), 3037–3072.

[27] Joshi, B.P., Mohanakrishnan, D., Mittal, G., Kar, S., Pola, J.K., Golakoti, N.R., Nanubolu, J.B., Rajesh Babu, D., Sai Suraj Kumar, S., and Sahal, D., 2018, Synthesis, mechanistic and synergy studies of diarylidenecyclohexanone derivatives as new antiplasmodial pharmacophores, *Med. Chem. Res.*, 27 (10), 2312–2324.

[28] Astuti, E., Raharjo, T.J., Manalu, P.B., Putra, I.S., Waskitha, S.S., and Solin, J., 2021, Synthesis, molecular docking, and evaluation of some new curcumin analogs as antimalarial agents, *Indones. J. Chem.*, 21 (2), 452–461.

[29] Salas, P.F., Herrmann, C., Cawthray, J.F., Nimphius, C., Kenkel, A., Chen, J., de Kock, C., Smith, P.J., Patrick, B.O., Adam, M.J., and Orvig, C., 2013, Structural characteristics of chloroquine-bridged ferrocenophane analogues of ferroquine may obviate malaria drug-resistance mechanisms, *J. Med. Chem.*, 56 (4), 1596–1613.

[30] Dambuza, N.S., Smith, P., Evans, A., Norman, J., Taylor, D., Andayi, A., Egan, T., Chibale, K., and Wiesner, L., 2015, Antiplasmodial activity, *in vivo* pharmacokinetics and anti-malarial efficacy evaluation of hydroxypyridinone hybrids in a mouse model, *Malar. J.*, 14 (1), 505.

[31] Chander, S., Tang, C.R., Al-Maqtari, H.M., Jamalis, J., Penta, A., Ben Hadda, T., Mohd Sirat, H., Zheng, Y.T., and Sankaranarayanan, M., 2017, Synthesis and study of anti-HIV-1 RT activity of 5-benzoyl-4-methyl-1,3,4,5-tetrahydro-2*H*-1,5-benzodiazepin-2-one derivatives, *Bioorg. Chem.*, 72, 74–79.

[32] Fatunde, O.A., and Brown, S.A., 2020, The role of CYP450 drug metabolism in precision cardio-oncology, *Int. J. Mol. Sci.*, 21 (2), 604.

[33] Al Sheikh Ali, A., Khan, D., Naqvi, A., Al-Blewi, F.F., Rezki, N., Aouad, M.R., and Hagar, M., 2021, Design, synthesis, molecular modeling, anticancer studies, and density functional theory calculations of 4-(1,2,4-triazol-3- ylsulfanylmethyl)-1,2,3-triazole derivatives, *ACS Omega*, 6 (1), 301–316.